



HAL
open science

Exacerbation of thrombo-inflammation by JAK2V617F mutation worsens the prognosis of cerebral venous sinus thrombosis.

Marie-Charlotte Bourrienne, Véronique Le Cam Duchez, Dorothée Faille, Carine Farkh, Mialitiana Solo Nomenjanahary, Juliette Gay, Stéphane Loyau, Clément Journée, Sébastien Dupont, Véronique Ollivier, et al.

► To cite this version:

Marie-Charlotte Bourrienne, Véronique Le Cam Duchez, Dorothée Faille, Carine Farkh, Mialitiana Solo Nomenjanahary, et al.. Exacerbation of thrombo-inflammation by JAK2V617F mutation worsens the prognosis of cerebral venous sinus thrombosis.. Blood Advances, inPress, 10.1182/bloodadvances.2023011692 . hal-04520587

HAL Id: hal-04520587

<https://hal.science/hal-04520587>

Submitted on 25 Mar 2024

HAL is a multi-disciplinary open access archive for the deposit and dissemination of scientific research documents, whether they are published or not. The documents may come from teaching and research institutions in France or abroad, or from public or private research centers.

L'archive ouverte pluridisciplinaire **HAL**, est destinée au dépôt et à la diffusion de documents scientifiques de niveau recherche, publiés ou non, émanant des établissements d'enseignement et de recherche français ou étrangers, des laboratoires publics ou privés.



Distributed under a Creative Commons Attribution 4.0 International License

Exacerbation of thrombo-inflammation by *JAK2*^{V617F} mutation worsens the prognosis of cerebral venous sinus thrombosis

Tracking no: ADV-2023-011692R1

Marie-Charlotte Bourrienne (INSERM U1148, LVTS, France) Véronique Le Cam Duchez (Normandie Univ, UNIROUEN, INSERM U1096, Rouen University Hospital, Vascular Hemostasis Unit, F 76000 Rouen, France, France) Dorothee Faille (Bichat Hospital, France) Carine Farkh (INSERM U1148, LVTS, France) Mialitiana Solonomenjanahary (INSERM U1148, France) Juliette Gay (Hôpital Bichat Claude Bernard, France) Stéphane Loyau (INSERM, CHU Bichat,) Clément Journé (INSERM U1148, LVTS, France) Sébastien Dupont (INSERM U1148, LVTS, France) Véronique Ollivier (INSERM, France) Jean-Luc Villeval (INSERM, U1287, Gustave Roussy, Université Paris Saclay, France) Isabelle Plo (INSERM UMR 1287, France) Valérie Edmond (INSERM U1287, France) Martine Jandrot-Perrus (University Paris Cité, France) Sylvie Labrousche-Colomer (University Bordeaux, INSERM, Biologie des maladies cardiovasculaires, U1034, F-33600 Pessac, France, France) Bruno Cassinat (Hopital Saint-Louis, Assistance Publique-Hopitaux de Paris, France) Emmanuelle Verger (APHP Hôpital St Louis, France) Jean-Philippe Desilles (Université Paris Cité, Inserm, UMRS-1144, Optimisation Thérapeutique en Neuropsychopharmacologie, F-75006 Paris, France) Benoît Ho Tin Noé (INSERM, U1148, France) Aude Triquenot Bagan (Rouen University Hospital, Department of Neurology and INSERM CIC-CRB 1404, F-76000 Rouen , France, France) Mikaël Mazighi (Université Paris Cité, Inserm, UMRS-1144, Optimisation Thérapeutique en Neuropsychopharmacologie, F-75006 Paris, France) Nadine Ajzenberg (AP-HP, INSERM, France)

Abstract:

Cerebral venous sinus thrombosis (CVST) is an uncommon venous thromboembolic event accounting for <1% of strokes resulting in brain parenchymal injuries. *JAK2*^{V617F} mutation, the most frequent driving mutation of myeloproliferative neoplasms has been reported to be associated with worse clinical outcomes in patients with CVST. We investigated whether hematopoietic *JAK2*^{V617F} expression predisposes to specific pathophysiological processes and/or worse prognosis after CVST. Using an in vivo mouse model of CVST, we analyzed clinical, biological and imaging outcomes in mice with hematopoietic-restricted *Jak2*^{V617F} expression, compared to *Jak2*^{WT} mice. In parallel, we studied a human cohort of *JAK2*^{V617F}-positive or negative CVST. Early after CVST, mice with hematopoietic *Jak2*^{V617F} expression had increased adhesion of platelets and neutrophils in cerebral veins located in the vicinity of CVST. On day 1, *Jak2*^{V617F} mice had a worse outcome characterized by significantly more frequent and severe intracranial hemorrhages (ICH) and higher mortality rates. Peripheral neutrophil activation was enhanced, as indicated by higher circulating platelet-neutrophil aggregates, upregulated CD11b expression, and higher myeloperoxidase (MPO) plasma level. Concurrently, immunohistological and brain homogenates analysis showed higher neutrophil infiltration and increased blood-brain-barrier disruption. Similarly, *JAK2*^{V617F}-positive CVST patients tended to present higher thrombotic burden and had significantly higher SII, a systemic thrombo-inflammatory marker, compared to *JAK2*^{V617F}-negative patients. In mice with CVST, our study corroborates that *Jak2*^{V617F} mutation leads to a specific pattern including increased thrombotic burden, ICH and mortality. The exacerbated thrombo-inflammatory response, observed both in mice and *JAK2*^{V617F}-positive patients, could contribute to hemorrhagic complications.

Conflict of interest: No COI declared

COI notes:

Preprint server: No;

Author contributions and disclosures: Conceptualization, MCB, NA and MM; Formal analysis, MCB, NA; Investigation, MCB, MS, CJ, CF; Resources, IP, JLV, VE, BC and EV; Writing - original draft, MCB, NA and MM.; Critical review, NA, MM, DF, and BHT. VLCD and ATB were the main investigators of the FPCCVT study. A complete list of the FPCCVT investigators appears in the "Appendix". All authors have read and agreed to the published version of the manuscript.

Non-author contributions and disclosures: No;

Agreement to Share Publication-Related Data and Data Sharing Statement: Requests for data sharing should be sent to Marie-Charlotte Bourrienne (marie-charlotte.bourrienne@inserm.fr).

Clinical trial registration information (if any): This study was registered at www.clinicaltrials.gov as #NCT02013635.

Exacerbation of thrombo-inflammation by *JAK2*^{V617F} mutation worsens the prognosis of cerebral venous sinus thrombosis

Running title: *JAK2*^{V617F} mutation and cerebral venous thrombosis

Marie-Charlotte Bourrienne^{1,2}, Véronique Le Cam Duchez³, Dorothee Faille^{1,2}, Carine Farkh^{1,2}, Mialitiana Solonomenjanahary⁴, Juliette Gay^{1,2}, Stéphane Loyau¹, Clément Journée⁵, Sébastien Dupont⁴, Véronique Ollivier⁴, Jean-Luc Villeval⁶, Isabelle Plo⁶, Valérie Edmond⁶, Martine Jandrot-Perrus¹, Sylvie Labrousche-Colomer⁷, Bruno Cassinat⁸, Emmanuelle Verger⁸, Jean-Philippe Desilles^{4,9}, Benoît Ho-Tin-Noé⁴, Aude Triquenot Bagan¹⁰, Mikael Mazighi^{4,11*}, Nadine Ajzenberg^{1,2*}.

On behalf of the FPCCVT Study Group.

¹ Université Paris Cité and Université Sorbonne Paris Nord, INSERM, UMRS-1148, LVTS, F-75018 Paris, France

² Laboratoire d'Hématologie, AP-HP, Hôpital Bichat-Claude Bernard, F-75018 Paris, France

³ Normandie Univ, UNIROUEN, INSERM U1096, Rouen University Hospital, Hemostasis Unit and INSERM CIC-CRB 1404, F-76000 Rouen, France

⁴ Université Paris Cité, Inserm, UMRS-1144, Optimisation Thérapeutique en Neuropsychopharmacologie, F-75006 Paris, France

⁵ Université Paris Cité, INSERM UMS34, Fédération de Recherche en Imagerie Multimodalités (FRIM), Faculté de Médecine X. Bichat, F-75018 Paris, France.

⁶ INSERM U1287, Gustave Roussy, Université Paris-Saclay, F-94800 Villejuif France.

⁷ Université de Bordeaux, INSERM U1034, Biologie des maladies cardio-vasculaires & Laboratoire d'hématologie, Centre Hospitalier Universitaire de Bordeaux, F-33604 Pessac, France.

⁸ Laboratoire de Biologie Cellulaire, AP-HP, Hôpital Saint-Louis, F-75010 Paris France.

⁹ Département de Neuroradiologie interventionnelle, Hôpital Fondation Rothschild, F-75019 Paris, France

¹⁰ Rouen University Hospital, Department of Neurology and INSERM CIC-CRB 1404, F-76000 Rouen, France

¹¹ Département de Neurologie, AP-HP, Hôpital Lariboisière, FHU NeuroVasc, F-75010 Paris, France.

Correspondence to:

Marie-Charlotte Bourrienne

Hôpital Bichat, AP-HP

Laboratory for Vascular Translational Science (LVTS), INSERM UMRS 1148

46 rue Henri Huchard, 75877 PARIS Cedex 18, France

Tel : 33 (0)1.40.25.85.21

E-mail : marie-charlotte.bourrienne@inserm.fr

Requests for data sharing should be sent to Marie-Charlotte Bourrienne (marie-charlotte.bourrienne@inserm.fr).

Abstract: 241 words

Text: 4026 words

Figures and Tables: 7

Supplemental Data: Yes

Reference count: 61

Key words: myeloproliferative disorders; JAK2V617F mutation; cerebral venous sinus thrombosis; intracerebral hemorrhage; mouse model

Key points:

- *JAK2*^{V617F} mutation contributes to hemorrhagic lesions and to mortality in an experimental model of cerebral venous thrombosis
- *JAK2*^{V617F} mutation exacerbates thrombo-inflammatory response during cerebral venous thrombosis

ABSTRACT

Cerebral venous sinus thrombosis (CVST) is an uncommon venous thromboembolic event accounting for <1% of strokes resulting in brain parenchymal injuries. *JAK2*^{V617F} mutation, the most frequent driving mutation of myeloproliferative neoplasms has been reported to be associated with worse clinical outcomes in patients with CVST. We investigated whether hematopoietic *JAK2*^{V617F} expression predisposes to specific pathophysiological processes and/or worse prognosis after CVST. Using an *in vivo* mouse model of CVST, we analyzed clinical, biological and imaging outcomes in mice with hematopoietic-restricted *Jak2*^{V617F} expression, compared to *Jak2*^{WT} mice. In parallel, we studied a human cohort of *JAK2*^{V617F}-positive or negative CVST.

Early after CVST, mice with hematopoietic *Jak2*^{V617F} expression had increased adhesion of platelets and neutrophils in cerebral veins located in the vicinity of CVST. On day 1, *Jak2*^{V617F} mice had a worse outcome characterized by significantly more frequent and severe intracranial hemorrhages (ICH) and higher mortality rates. Peripheral neutrophil activation was enhanced, as indicated by higher circulating platelet-neutrophil aggregates, upregulated CD11b expression, and higher myeloperoxidase (MPO) plasma level. Concurrently, immunohistological and brain homogenates analysis showed higher neutrophil infiltration and increased blood-brain-barrier disruption. Similarly, *JAK2*^{V617F}-positive CVST patients tended to present higher thrombotic burden and had significantly higher SII, a systemic thrombo-inflammatory marker, compared to *JAK2*^{V617F}-negative patients.

In mice with CVST, our study corroborates that *Jak2*^{V617F} mutation leads to a specific pattern including increased thrombotic burden, ICH and mortality. The exacerbated thrombo-inflammatory response, observed both in mice and *JAK2*^{V617F}-positive patients, could contribute to hemorrhagic complications.

INTRODUCTION

Cerebral sinus-venous thrombosis (CVST) is an atypical site of venous thromboembolism (VTE). It represents an uncommon form of stroke with high-variably clinical course that mainly affects young adults.¹ CVST leads to impaired venous drainage, intracranial hypertension and parenchymal lesions including cerebral edema, ischemia, intracerebral haemorrhage (ICH) reported in up to 40%.²⁻⁶ In CVST, since the thrombosis initiation depends largely on the presence of prothrombotic conditions (acquired and inherited thrombophilia, trauma...) the underlying causes cannot be identified in 15-30% of cases.^{2-4,6}

Several small series have suggested that CVST may represent the first clinical manifestation of Bcr/Abl-negative myeloproliferative neoplasms (MPNs), both in overt or “occult” MPNs (i.e. without any biological/clinical signs of MPNs).⁷ The gain-of-function $JAK2^{V617F}$ mutation is the main molecular hallmark of MPNs, whose prevalence is estimated from 2.6 to 3.9%.^{8,9} Hence, while $JAK2^{V617F}$ mutation is a leading cause of splanchnic veins thrombosis (25-35%), another atypical location of VTE, its relationship to CVST remains unclear and systematic screening in routine diagnostic work-up is not recommended.^{5,9,10} Nevertheless, early diagnosis of MPNs during CVST could have critical therapeutic implications. In CVST, malignancies including MPNs are associated with an increased risk of thrombotic recurrence,¹¹⁻¹³ ICH,¹⁴ and poor neurological outcome.^{2,4,15,16}

Clinical studies have demonstrated that myeloid $JAK2^{V617F}$ expression is associated with increased risk for thrombotic complications and cardiovascular events.¹⁷ Accordingly, $Jak2^{V617F}$ mice have shown their propensity to thrombosis in previous venous thrombosis models such as $FeCl_3$ -injury to mesenteric veins,¹⁸ inferior vena cava ligation,^{19,20} or acute pulmonary embolism.²¹ $JAK2^{V617F}$ -driven pathophysiological mechanisms includes abnormal cell interactions, changes in the inflammatory environment and rheological properties that switch cells from a resting to a pro-thrombotic and pro-inflammatory phenotype.¹⁷ Numerous studies have provided evidence that the pathogenesis of MPN-related thrombosis involves platelet and neutrophil activation.²²⁻²⁴ Moreover, enhanced $JAK2^{V617F}$ neutrophil infiltration has been incriminated in accelerated vascular remodelling.²⁵⁻²⁷

During CVST, while parenchymal lesions are critical for neurological outcome, predictive factors for their development, especially in MPNs, are still largely elusive.^{15,28} Using *in vivo* two-photon imaging, Santisakultarm *et al* showed, in

hematopoietic $Jak2^{V617F}$ transgenic mice, increased adhesion of blood cells in cerebral microcirculation which where mainly constitute of platelet and neutrophil aggregates.³¹ These observations raise the possibility that hematopoietic expression of $JAK2^{V617F}$ enhance brain parenchymal injury, thus worsening CVST through an *in vivo* thrombo-inflammatory process. To date, human studies have mainly focused on $JAK2^{V617F}$ as a risk factor for CVST rather than on its pathophysiological related process.

Using a mouse knock-in (KI) model of MPNs with specific hematopoietic $Jak2^{V617F}$ expression, we investigated whether $Jak2^{V617F}$ expression contributes to CVST-related parenchymal injury. Specifically, we examined the role of thrombo-inflammation, focusing on neutrophils and platelets. We also investigated whether the presence of $JAK2^{V617F}$ mutation could affect clinical outcome and levels of circulating thrombo-inflammatory markers in a human cohort of CVST.

METHODS

Animal experiments

We used a well characterized hematopoietic *Jak2*^{V617F} KI model.^{18,32} Briefly, bone marrow (BM) cells (3×10^6 cells) from *Jak2*^{V617F} KI/VavCre mice were engrafted into 6- to 8-week-old C57BL/6J mice that had undergone lethal total body irradiation thus resulting in polycythemia vera (PV)-like disease. Irradiated C57BL/6 mice transplanted with *Jak2*^{WT} BM cells (control littermate) were used as controls. Medullar reconstitution was allowed for 9 weeks before experiments were performed. This procedure ensures heterozygous expression of *Jak2*^{V617F} in all hematopoietic cells and minimizes the risk of *Jak2*^{V617F} expression in non-hematopoietic cells. Given that CVST is more likely to occur in women, we used female mice in all experiments. All animal procedures were carried out according guidelines formulated by the European Community for experimental animal use (L358-86/609EEC) under approval of the Committee on the Ethics of Animal Experiments (Paris Nord n°121, approval number n°14070). Animal experiments were performed using the animal facilities of the INSERM (APAFIS #2344-2016101015023392).

Mouse model for CVST

Superior sagittal sinus (SSS) thrombosis was performed using a thrombus-injected CVST model as described.³³ Briefly, standardized whole blood clots were formed one-day prior surgery using 1 UI/mL thrombin (Dade Behring Thrombin reagent, Siemens, Marburg, Germany) and 10mM CaCl₂. Mice were anesthetized using isoflurane gas in ambient air (4% for induction, 1.5% for maintenance). After craniotomy, clot was injected into SSS after careful puncture. Clot injection was combined with bilateral external jugular vein ligation in the CVST group. The sham group consisted in isolated craniotomy of age-matched mice. All mice were subjected to a neurological sensory-motor evaluation 1 day prior to and the 1st day post-surgery in a blinded fashion as described.³³ Neurological assessment and evolution at day 1 was expressed as a percentage of the basal neurological score.

Real-time intravital imaging of cortical circulation

Two hours after CVST, mice anesthetized using isoflurane gas (1.5% for maintenance) were injected with fluorescent tracers through the retro-orbital venous sinus, and placed under a fluorescence microscope (MacroFluo; Leica

Microsystems) equipped with a thermostated heating plate and connected to a scientific CMOS camera (ORCAFlash4.0; Hamamatsu Photonics, Japan). All circulating leukocytes/platelets were stained with rhodamine 6G (3 mg/kg, Sigma). Specific neutrophils observation was performed using Alexa Fluor 647-conjugated rat anti-mouse Ly6G (0.1 mg/kg, clone 1A8, BD Pharmingen). Vascular network was visualized using 2000 kDa FITC-Dextran (10 mg/kg, Sigma, St Louis, MO). Images were acquired using Metamorph software (Molecular Devices) and analyzed using ImageJ software (National Institutes of Health).

Magnetic resonance imaging

On post-operative day 1 (D1), magnetic resonance imaging (MRI) was performed on a Pharmascan 7-Tesla small animal scanner equipped using a mouse brain volume coil (Bruker, Ettlingen, Germany). Ischemic and haemorrhagic volume were calculated using Horos software as previously described (Supplemental material).³³

Immunohistochemical analyses

On D1 post-surgery, mice were sacrificed by trans-cardiac infusion of ice-cold phosphate-buffered saline (PBS, pH: 7.4) followed by zinc fixative. Brains were removed from skulls, divided into 4 segments. Macroscopic examination of brain (adapted from *Egashira et al*³⁴) was used to assign a grade from 0 to 2 depending on the severity of ICH as follows: 0, no ICH; 1: localized/minimal ICH; 2 : diffuse/deep parenchymal ICH . Then, brains were preserved in zinc fixative for at least 24 hours, before being processed and stained (Supplemental Material).

Assessment of brain and plasma levels of thrombo-inflammatory markers

Plasma levels of soluble P-Selectin (sPSel), MPO and platelet factor 4 (PF4) were measured using ELISA kits (R&D Systems, Cat# MPS00, DY3667 and DY595 respectively). Adapted from³⁵, quantification of citrullinated histone H3 bound DNA (H3Cit-DNA) was performed using an anti-histone H3 (Cat. #5103, Abcam) antibody following by fluorescent Quant-iT Picogreen dsDNA assay (Invitrogen) to detect DNA. For measurements in brain homogenates, brains were recovered after intracardiac perfusion of ice cold PBS. MPO, PF4, IgG and hemoglobin were measured using different ELISA kits (HycultBiotech, Cat#HK210; R&D Systems Cat# DY595; Abcam

Cat#ab151276 and Cat#ab157715; respectively). A thrombo-inflammatory score, the systemic immune-inflammation index (SII index: [Platelet, $\times 10^9/L$ x Neutrophil, $\times 10^9/L$] / [Lymphocyte, $\times 10^9/L$]) was calculated in mice from blood cell counts, as described previously.³⁶

Assessment of platelet-neutrophil aggregates (PNA) and platelet activation by flow cytometry

PNA and platelet activation were measured in heparinized (15 UI/mL) unstimulated whole blood before and one day after CVST using BD Accuri™ C6 Flow Cytometer (BD Biosciences, San Jose, USA). Combination of rat anti-mouse CD45-PerCP-Cy5.5 (30F11, Biolegend), Ly6G-AF555 (1A8, BD Biosciences), CD11b-AF488 (M1 170, Biolegend) was used for labelling leukocytes and neutrophils. Rat anti-mouse CD42a-AF647 (GPIX) (M051-0, Emfret) was used to label platelets. A minimum of 500 000 events was recorded. The percentage of CD45+/CD42a+ double-positive events representing platelet-leukocyte aggregates was recorded. Within platelet-leukocyte aggregates, PNAs were identified from Ly6G positive events as the percentage of neutrophils.

Platelet activation was measured using surface exposure of P-Selectin (rat anti-mouse CD62P-PE, RMP1, Biolegend). Activation of $\alpha_{IIb}\beta_3$ integrin (GPIIb/IIIa) was detected using binding of FITC labelled-fibrinogen (30 $\mu\text{g/mL}$).

Human case-control study

On behalf of the prospective CVST French cohort study (FPCCVT) investigators,⁶ we retrospectively analyzed patients for whom peripheral blood DNA was available for *JAK2*^{V617F} mutation screening. Genomic DNA was extracted using an automated standard procedure from whole blood collected by venipuncture on EDTA and stored at -80°C until analysis. *JAK2*^{V617F} mutation was screened using high-resolution melting (HRM) analysis on LightCycler 480 instrument (Roche Diagnostics, Rotkreuz, Switzerland). Allelic burden was determined in *JAK2*^{V617F}-positive cases using the Ipsogen *JAK2* MutaQuant kit (Qiagen, Courtaboeuf, France) according to manufacturer's instructions. *JAK2*^{V617F}-positive MPNs were diagnosed according the 2022 World Health Organization diagnostic criteria.³⁷

Demographic, clinical, imaging and biological (including the SII) data were compared between $JAK2^{V617F}$ -positive and -negative CVST at baseline and after 3 months of follow-up. In addition, plasma levels of MPO (#DY3174, R&D Systems) were measured according to manufacturer's instruction.

Statistical analysis

Statistical analysis of differences between groups was performed using the appropriate test as indicated. A P value <0.05 was considered significant.

Data sharing statement

Requests for data sharing should be sent to Marie-Charlotte Bourrienne (marie-charlotte.bourrienne@inserm.fr).

RESULTS

$Jak2^{V617F}$ mutation exacerbates early vascular recruitment of neutrophils and platelets, two hours after CVST

We used a mouse model of MPN characterized by hematopoietic $Jak2^{V617F}$ expression resulting in a variant allele frequency (VAF) of 50% in all hematopoietic lineages, as previously described.³² Compared to $Jak2^{WT}$, $Jak2^{V617F}$ mice displayed a PV-like phenotype, with higher haemoglobin level, neutrophil count (Supplemental Table S2) and enlarged spleen (spleen weight 296 ± 74 vs 66 ± 15 mg, $p<0.001$).

Intravital microscopy was performed 2 hours after injection of standardised autologous thrombi into the SSS (Figure 1). Sham-operated mice ($Jak2^{V617F}$ and $Jak2^{WT}$) exhibited sparse adherent leukocytes and platelets within venous compartment (Figure 1B). After CVST, rolling and firm adhesion of leukocytes and platelets was observed along venous vessels (SSS, cortical veins, venules). Adhesion of leukocytes and platelets appeared to be more pronounced in $Jak2^{V617F}$ mice compared to $Jak2^{WT}$ counterparts (Figure 1BC; Video 1). Accordingly, quantification of intravascular rhodamine-associated fluorescence intensity was significantly higher in $Jak2^{V617F}$ compared to $Jak2^{WT}$ and sham-operated mice (Figure 1C). In $Jak2^{V617F}$ mice, Ly6G labelling indicated a greater level of neutrophil adhesion to the venous wall compared to $Jak2^{WT}$ mice (Figure 1D). At this stage, no extravasation of neutrophils or 2000 kD-FITC dextran reflecting BBB leakage was

observed into parenchyma.

In all mice after CVST, dextran imaging showed black segments within venules, indicating a disruption in blood flow and formation of new thrombi at a distance from the original site (Figure 1B, Video 1). Venular occlusion appeared to be notably increased in *Jak2*^{V617F} compared to *Jak2*^{WT} mice.

CVST specificities in *Jak2*^{V617F} mice at D1

The role of *Jak2*^{V617F} mutation in CVST-related brain injury was assessed at D1 after SSS thrombosis. MRI showed small brain ischemic infarcts, without any difference in volume between *Jak2*^{WT} and *Jak2*^{V617F} mice (Figure 2AB). In contrast, *Jak2*^{V617F} mice had larger MRI ICH volumes ($p < 0.05$) and higher brain haemoglobin levels ($p < 0.05$) than *Jak2*^{WT} mice (Figure 2ABC). Accordingly, brain macroscopic examination showed that incidence of ICH was twofold higher in *Jak2*^{V617F} mice ($n = 13/17$) compared to *Jak2*^{WT} mice ($n = 5/12$). Interestingly, *Jak2*^{V617F} mice showed increased severity of ICH, compared to *Jak2*^{WT} mice, ranging from localised (type 1) to deep parenchymal ICH (type 2) (Figure 2D). Type 2 ICH, the most severe pattern, was observed in 41% of *Jak2*^{V617F} mice ($n = 7/17$), and never in *Jak2*^{WT} mice (Figure 2E). Among *Jak2*^{V617F} mice, blood hemoglobin levels were not significantly different between mice with no, type 1 and type 2 ICH.

At D1 post-CSVT, survival rate was significantly reduced in *Jak2*^{V617F} mice ($n = 13/17$) compared to *Jak2*^{WT} counterparts ($n = 12/12$) ($p = 0.044$) although the neurological score did not differ between *Jak2*^{WT} and *Jak2*^{V617F} mice (-17.9 and -20.1% compared from baseline, respectively). Sham-operated mice did not present any brain injury irrespective of *Jak2* mutation status (data not shown).

Thrombosis expansion in *Jak2*^{V617F} mice at D1

Consistent with *in vivo* imaging, fluorescent staining of brain sections from *Jak2*^{WT} and *Jak2*^{V617F} mice confirmed the presence of fibrin deposits with a vascular pattern away from the SSS after CVST, suggesting new intravascular thrombi (Supplemental data, Figure S1). In addition, *Jak2*^{V617F} mice showed more diffuse intravascular fibrin deposits compared to *Jak2*^{WT} mice.

BBB disruption in *Jak2*^{V617F} mice at D1

Next, we assessed BBB integrity by measuring IgG in whole brain homogenates at D1 (Figure 3). While brain IgG levels in CVST were significantly increased in both types of mice compared to the sham-operated group, significantly higher IgG levels were observed in *Jak2*^{V617F} compared to *Jak2*^{WT} mice ($p < 0.05$) (Figure 3B). In brain sections, IgG extravasation was observed both in haemorrhagic and non-haemorrhagic areas around vessels, but to a greater extent in *Jak2*^{V617F} mice compared to *Jak2*^{WT} mice (Figure 3A).

At D1 after CVST, *Jak2*^{V617F} mutation is associated with brain neutrophil infiltration

We further investigated whether the *Jak2*^{V617F} mutation affects neutrophil and platelet parenchymal infiltration at D1 after CVST (Figure 4). No platelet accumulation was observed in either type of mice (data not shown). In both types of mice, CVST induced a parenchymal neutrophil infiltration, in non-hemorrhagic and hemorrhagic cortical areas, compared to sham-operated mice, which was significantly increased in *Jak2*^{V617F} mice compared to *Jak2*^{WT} mice (Figure 4ABC). We did not observe neutrophils stained positive for citrullinated histone H3 (H3Cit) (data not shown). PF4 and MPO in brain homogenates were measured as indicators of platelet and neutrophil infiltration, respectively (Figure 4DE). At D1 after CVST, only *Jak2*^{V617F} mice had significantly elevated MPO levels (Figure 4E).

In *Jak2*^{V617F} mice, CVST was associated with higher circulating platelet-neutrophil aggregates (PNA) levels and neutrophils activation

Due to the exacerbated neutrophils infiltration in brain parenchyma from *Jak2*^{V617F} mice after CVST, we investigated neutrophil activation in whole blood at D1 (Figure 5). In line with the MPN phenotype, circulating neutrophil count was increased in *Jak2*^{V617F} mice compared to *Jak2*^{WT} irrespective of the experimental conditions (Supplemental Table S2). Circulating PNA levels and neutrophil CD11b expression were significantly increased at baseline and D1 after CVST in *Jak2*^{V617F} mice compared to *Jak2*^{WT} mice (Figure 5AB). Then, we compared plasma MPO levels as a biomarker of neutrophil activation and degranulation (Figure 5C). *Jak2*^{V617F} mice with CVST had significantly higher MPO levels compared to baseline conditions, but not compared to sham-operated *Jak2*^{V617F} mice. After correction for neutrophil count, no significant difference in MPO levels was observed between *Jak2*^{WT} and *Jak2*^{V617F}

mice with CVST or sham-operated mice (data not shown). Plasma levels of H3Cit-DNA, used as a biomarker for the release of Neutrophil extracellular traps (NETs), tended to be higher in *Jak2*^{V617F} mice compared to *Jak2*^{WT} mice after CVST ($p=0.06$) (Figure 5D).

In order to assess platelet activation, we measured surface P-Selectin and activated α IIb β 3 integrin on circulating platelets (Figure 6). While *Jak2*^{WT} and *Jak2*^{V617F} mice expressed similar level of activated α IIb β 3 integrin, P-Selectin expression was significantly decreased in *Jak2*^{V617F} mice compared to *Jak2*^{WT} mice, with no difference between sham-operated and CSVT mice (Figure 6B). Concurrently, soluble P-Selectin levels were significantly higher in *Jak2*^{V617F} mice compared to their *Jak2*^{WT} counterparts while platelet counts were similar (Figure 6C; Supplemental Data, Table S2). The same pattern was observed using another biomarker of platelet α -granule, soluble PF4, (Supplemental Data, Figure S2). The thrombo-inflammatory marker, SII, was significantly increased from baseline to D1 after CVST, regardless of *Jak2* mutation status (Supplemental data, Table S2). However, after CVST, SII was significantly higher in *Jak2*^{V617F} mice than in their *Jak2*^{WT} counterparts ($p<0.01$).

***JAK2*^{V617F} mutation specificities in a human cohort**

To assess the clinical relevance of *JAK2*^{V617F} mutation in CVST, we analysed its prevalence in 216 patients with CVST from the prospective CVST French cohort study (FPCCVT).⁶ *JAK2*^{V617F} mutation was detected in 4.2% of CVST patients (i.e. *JAK2*^{V617F}-positive CVST; $n=9$, all female) with a VAF ranging from 4 to 81% (Supplemental Table S3). Clinical, biological and radiological characteristics of patients with *JAK2*^{V617F}-positive and -negative CVST were depicted in Table 1.

Among *JAK2*^{V617F}-negative patients, 24% had inherited thrombophilia, which did not significantly alter the thrombotic burden and outcome of CVST compared to those without thrombophilia. Among *JAK2*^{V617F}-positive patients, 5 had a “non-overt” MPN with normal blood counts, while the other 4 had abnormal blood cell counts (Supplemental Table S3). None of these patients was receiving antithrombotic or cytoreductive therapy at the time of enrolment. Compared to *JAK2*^{V617F}-negative CVST patients, those harbouring *JAK2*^{V617F} mutation tended to present higher neutrophil count ($p=0.055$). Apart from the use of oestrogen contraceptives in 4 out of 9 patients with *JAK2*^{V617F} mutation, no other risk factor was observed in these

patients. CVST thrombus load (i.e. combined sinus and vein thrombosis) tended to increase in *JAK2*^{V617F}-positive compared to negative CVST patients (66.6% vs 35.7%, p=0.079). In *JAK2*^{V617F}-positive patients, the SII was significantly higher compared to *JAK2*^{V617F}-negative patients (p=0.019). As experimental data from *Jak2*^{V617F} mice indicated enhanced neutrophil activation following CVST, we also measured plasma MPO levels in CVST patients. A trend towards higher MPO levels was observed in *JAK2*^{V617F}-positive CVST compared to negative CVST (Table 1).

DISCUSSION

Using an original CVST mouse model and a human cohort of patients with CVST, our study provides new data pointing to a role for thrombo-inflammation in the pathophysiology of *JAK2*^{V617F}-positive CVST. In *Jak2*^{V617F} mice, CVST was characterized by widespread thrombosis, more severe ICH with higher mortality, increased BBB permeability and higher circulating PNA aggregates. Interestingly, *JAK2*^{V617F}-positive patients with CVST and *Jak2*^{V617F} mice presented significantly higher levels of the SII thrombo-inflammatory biomarker as compared to their counterparts.

From a mechanistic point of view, we observed that *Jak2*^{V617F} mice had (1) increased neutrophil and platelet adhesion to the venous wall, (2) blood flow disturbance within venules and (3) increased microvascular fibrin deposits remotely from the initial CVST site compared to *Jak2*^{WT} mice. In line with previous venous thrombosis models, we show that *Jak2*^{V617F} promotes propagation and extension of thrombosis.^{18–21} In our model, while ischemic lesions were similar between mice, ICH was more frequent and severe in *Jak2*^{V617F} mice than in *Jak2*^{WT} mice. As reported in human CVST, ICH was likely responsible for the higher mortality observed in *Jak2*^{V617F} mice.^{14,16,38} Together, these observations support the pathophysiological link between thrombosis and ICH in CVST.^{39,40} Indeed, as the thrombus expands in the venous circulation and its collaterals, intravenous pressure rises, potentially leading to BBB disruption, edema, and subsequent ICH.

Our study was based on a *Jak2*^{V617F} KI mouse model in which the previously reported bleeding phenotype¹⁸ may have contributed to worsening ICH. Particularly, these mice presented a haemostatic defect characterized by (1) a mild collagen GPVI receptor deficiency, (2) low platelet activation response to GPVI, CLEC-2 and thrombin receptor agonists, (3) decreased content in large vWF multimers responsible for acquired von Willebrand syndrome (AVWS).¹⁸ In our study, no additional bleeding was observed in sham-operated *Jak2*^{V617F} mice compared to *Jak2*^{WT} mice, suggesting that haemostatic abnormalities alone do not explain the bleeding phenotype. These data support a scenario where *Jak2*^{V617F} promotes ICH through increased thrombotic burden of CVST rather than isolated haemostatic defect.

We hypothesize that dysregulated and excessive interplay between platelets and neutrophils may contribute to promote thrombus expansion that predispose *Jak2*^{V617F} mice to develop vascular permeability and ICH. In line with this hypothesis, *Jak2*^{V617F} mice had higher circulating PNA levels and upregulated membrane expression of neutrophil CD11b, compared to *Jak2*^{WT} mice, after CVST. CD11b, a marker of neutrophil activation, is a member of β 2-integrin (associated with CD18), which is known to interact with the platelet GPIb receptor. Our data strengthen previous findings, using *in vivo* mouse models, that showed abnormal activation of the β 1/ β 2 integrin signaling pathway in *Jak2*^{V617F} neutrophils, promoting their interaction with endothelium and platelets, as well as venous thrombosis.^{20,27} Moreover, we observed an increase in PF4 and soluble P-Selectin levels, independent of CVST and platelet count, that likely indicates platelet activation in *Jak2*^{V617F} mice as reported in *JAK2*^{V617F} patients.⁴¹ Together, these data suggests that increased interaction of neutrophils with platelets in *Jak2*^{V617F} mice promote CVST expansion.^{24,41,42}

Enhanced platelet-neutrophil interaction is also known to favor activation of the coagulation cascade through neutrophil activation, release of proteases and NETs.^{43,44} In hematopoietic MPN models, it was previously reported that activated *Jak2*^{V617F} neutrophils are more prone to form NETs, particularly after interaction with *Jak2*^{V617F} platelets.^{19,21,45} In our study, plasma levels of H3Cit-DNA, a marker of NETs, tended to be higher in *Jak2*^{V617F} mice than in *Jak2*^{WT} mice only after CVST. No significant difference was observed in brain parenchyma. In line with upregulated CD11b expression, these results suggest that CVST induced a higher systemic neutrophil activation in *Jak2*^{V617F} mice that could promote NETs formation. In a *VavCre/Jak2*^{V617F} MPN model, higher levels of NETs and thrombosis rates were observed after partial ligation of inferior vena cava.¹⁹ Outside the context of MPN, pro-thrombotic effect of NETs has also been described in CVST patients compared to controls *via* fibrinolytic resistance and pro-coagulant changes in the endothelium.⁴⁶ Thus, the specificity of NETs and their role in the initiation and progression of CVST associated with *Jak2*^{V617F} need to be addressed in further studies.

In *Jak2*^{V617F} mice, PNA could also drive neutrophil migration across the endothelium, where it can cause vascular injury through the release of reactive oxygen species, proteolytic enzymes and chemokines.^{47,48} Consistent with this important role of neutrophils, Nagai *et al.* demonstrated that both CD18 immuno-neutralization and neutropenia rescue BBB permeability in a FeCl₃-injury CVST model.⁴⁹ In our study,

we observed the presence of extravasated IgG and neutrophils in non-haemorrhagic areas in parenchyma of *Jak2*^{V617F} mice suggesting that a compromised BBB is a putative precursor to ICH. Taken together, these data support a scenario in which enhanced neutrophil-platelet interaction, as part of the thrombo-inflammatory response, may predispose *Jak2*^{V617F} mice to develop ICH by increasing the propensity for thrombus expansion and BBB permeability.

In the FPCCVT human cohort, we confirm that *JAK2*^{V617F} mutation is associated to CVST in ≈4% of cases^{8,9} with a female preponderance and a heterogeneous biologic profile ranging from overt to “occult” MPNs.^{8,51–53} As a result of this heterogeneity, the median blood count parameters were not significantly elevated in *JAK2*^{V617F}-positive CVST patients compared to negative patients. Conflicting data exist regarding the specificity of *JAK2*^{V617F}-positive CVST, either indicating an increased thrombotic burden, risk of ICH and mortality^{14,16,38,54} or a good prognosis.^{51,52} Consistent with our experimental data, *JAK2*^{V617F}-positive patients tended to have a higher thrombosis load and had an increased SII compared to negative patients. In contrast to *Li et al*, we did not observe an association between higher SII and worse prognosis of CVST in these patients.³⁶ Nevertheless, our findings suggest that an exacerbated thrombo-inflammatory response may predispose *JAK2*^{V617F} patients to extensive CVST with a higher risk of ICH. Thus, early curative anticoagulation at the onset of diagnosis may be critical in these patients to stop the thrombosis process and reduce the risk of ICH, as recommended.^{5,10}

Nevertheless, some limitations need to be underlined. In the FPCCVT cohort, the rate of severe clinical presentation (ICH, coma) was lower than in previous studies, so it is possible that this latter cohort does not cover the full clinical spectrum of CVST.^{4,6} In addition, the small sample size of *JAK2*^{V617F}-positive patients likely limits the power of statistical analysis. For experimental study, we used lethally irradiated recipient mice engrafted with bone marrow from *Jak2*^{V617F} KI/VavCre to restrict expression to hematopoietic cells but not ECs. Thus, *Jak2*^{V617F} mutation was not expressed in endothelial cells which have been previously shown to be pro-thrombotic.^{55,56} In this model, the possibility that RBC could contribute to CVST expansion and ICH should be considered through increased (i) adhesion to endothelial laminin, (ii) upregulation of pleckstrin 2, (iii) secretion of erythrocyte-derived microvesicles contributing to oxidative stress.^{57–59} Nevertheless, in *Jak2*^{V617F} mice, we did not observe a relationship between hemoglobin levels and the incidence

or severity of ICH. This suggests that increased viscosity and rheological changes may probably not play a major role in the development of ICH in our model.

Although the phenotype is also PV-like, this model results in a VAF of 50% in all hematopoietic lineages rather than a few hematopoietic stem cells as in the *PF4iCre; Jak2^{V617F/WT}* model.⁶⁰ To go further, competitive transplants of normal and *Jak2^{V617F}* bone marrow cells at different ratios could be performed to study the impact of increasing VAF in CVST, as observed in patients (4 to 81%). Neutrophil and platelet specific MPN models without polycythemia (such as MRP8-iCre; *Jak2^{V617F}* and PF4-Cre/*JAK2^{V617F}* transgenic mice, respectively)^{45,61} or blockade strategy would be also helpful to confirm the mechanistic link between thrombo-inflammation and ICH during *Jak2^{V617F}*-positive CVST.

Thrombo-inflammation processes represent a new biological target for innovative therapeutic strategies to reduce disability and mortality occurring during the course of *JAK2^{V617F}*-related MPN diseases. Further studies are warranted to specifically address the respective roles of neutrophils and platelets in *JAK2^{V617F}*-related CVST brain damage.

ACKNOWLEDGMENTS

We are grateful to the French Intergroup Myeloproliferative (FIM).

Authors would like to thank Odile Vandapel, Céline André and Dr Muriel Quillard-Muraine, members of INSERM CIC-CRB U1404, CHU de Rouen, for their help in receiving, controlling, preparing, preserving and making available the human biological resources studied in this work and the “Direction de la Recherche Clinique et de l’Innovation” of Rouen University Hospital for the clinical data base of the FPCCVT.

A special thank you goes to all investigators of the FPCCVT study.

AUTHORSHIP CONTRIBUTIONS

Conceptualization, MCB, NA and MM; Formal analysis, MCB, NA; Investigation, MCB, MS, CJ, CF, SLC; Resources, IP, JLV, VE, BC and EV; Writing – original draft, MCB, NA and MM.; Critical review, NA, MM, DF, MJP and BHT. VLCD and ATB were the main investigators of the FPCCVT study. A complete list of the FPCCVT investigators appears in the “Appendix”. All authors have read and agreed to the published version of the manuscript.

CONFLICTS OF INTEREST

The authors declare no competing financial interests

FUNDING

This study was funded through a clinical research program (N° 2010/087/HP) of the French Ministry of Health. Dr Bourrienne is the recipient of a grant poste d'accueil INSERM. This study was supported by INSERM.

REFERENCES

1. Bousser M-G, Ferro JM. Cerebral venous thrombosis: an update. *Lancet Neurol.* 2007;6(2):162–170.
2. Duman T, Uluduz D, Midi I, et al. A Multicenter Study of 1144 Patients with Cerebral Venous Thrombosis: The VENOST Study. *J. Stroke Cerebrovasc. Dis.* 2017;26(8):1848–1857.
3. Ferro JM, Lopes MG, Rosas MJ, Ferro MA, Fontes J. Long-Term Prognosis of Cerebral Vein and Dural Sinus Thrombosis. *Cerebrovasc. Dis.* 2002;13(4):272–278.
4. Ferro JM, Canhão P, Stam J, Bousser M-G, Barinagarrementeria F. Prognosis of Cerebral Vein and Dural Sinus Thrombosis: Results of the International Study on Cerebral Vein and Dural Sinus Thrombosis (ISCVT). *Stroke.* 2004;35(3):664–670.
5. Saposnik Gustavo, Barinagarrementeria Fernando, Brown Robert D., et al. Diagnosis and Management of Cerebral Venous Thrombosis. *Stroke.* 2011;42(4):1158–1192.
6. Triquenot Bagan A, Crassard I, Drouet L, et al. Cerebral Venous Thrombosis: Clinical, Radiological, Biological, and Etiological Characteristics of a French Prospective Cohort (FPCCVT)—Comparison With ISCVT Cohort. *Front. Neurol.* 2021;0.:
7. Passamonti SM, Biguzzi E, Cazzola M, et al. The JAK2 V617F mutation in patients with cerebral venous thrombosis. *J. Thromb. Haemost.* 2012;10(6):998–1003.
8. Lamy M, Palazzo P, Agius P, et al. Should We Screen for Janus Kinase 2 V617F Mutation in Cerebral Venous Thrombosis? *Cerebrovasc. Dis.* 2017;44(3-4):97–104.
9. Dentali F, Squizzato A, Brivio L, et al. JAK2V617F mutation for the early diagnosis of Ph- myeloproliferative neoplasms in patients with venous thromboembolism: a meta-analysis. *Blood.* 2009;113(22):5617–5623.
10. Ferro JM, Bousser M-G, Canhão P, et al. European Stroke Organization guideline for the diagnosis and treatment of cerebral venous thrombosis - endorsed by the European Academy of Neurology. *Eur. J. Neurol.* 2017;24(10):1203–1213.
11. Miranda B, Ferro JM, Canhão P, et al. Venous thromboembolic events after cerebral vein thrombosis. *Stroke.* 2010;41(9):1901–1906.
12. Lim HY, Ng C, Donnan G, Nandurkar H, Ho P. Ten years of cerebral venous thrombosis: male gender and myeloproliferative neoplasm is associated with

thrombotic recurrence in unprovoked events. *J. Thromb. Thrombolysis*. 2016;42(3):423–431.

13. Palazzo P, Agius P, Ingrand P, et al. Venous Thrombotic Recurrence After Cerebral Venous Thrombosis: A Long-Term Follow-Up Study. *Stroke*. 2017;48(2):321–326.

14. Afifi K, Bellanger G, Buyck P-J, et al. Features of intracranial hemorrhage in cerebral venous thrombosis. *J. Neurol*. 2020;267(11):3292–3298.

15. Ferro JM, Bacelar-Nicolau H, Rodrigues T, et al. Risk Score to Predict the Outcome of Patients with Cerebral Vein and Dural Sinus Thrombosis. *Cerebrovasc. Dis*. 2009;28(1):39–44.

16. Porceddu E, Rezoagli E, Poli D, et al. Sex-related characteristics of cerebral vein thrombosis: A secondary analysis of a multicenter international cohort study. *Thromb. Res*. 2020;196:371–374.

17. Wolach O, Shacham Abulafia A. Can Novel Insights into the Pathogenesis of Myeloproliferative Neoplasm-Related Thrombosis Inform Novel Treatment Approaches? *Hemato*. 2021;2(2):305–328.

18. Lamrani L, Lacout C, Ollivier V, et al. Hemostatic disorders in a JAK2V617F-driven mouse model of myeloproliferative neoplasm. *Blood*. 2014;124(7):1136–1145.

19. Wolach O, Sellar RS, Martinod K, et al. Increased neutrophil extracellular trap formation promotes thrombosis in myeloproliferative neoplasms. *Sci. Transl. Med*. 2018;10(436.):

20. Edelmann B, Gupta N, Schnoeder TM, et al. JAK2-V617F promotes venous thrombosis through $\beta 1/\beta 2$ integrin activation. *J. Clin. Invest*. 2018;128(10):4359–4371.

21. Craver BM, Ramanathan G, Hoang S, et al. N-acetylcysteine inhibits thrombosis in a murine model of myeloproliferative neoplasm. *Blood Adv*. 2020;4(2):312–321.

22. Barbui T, Finazzi G, Falanga A. Myeloproliferative neoplasms and thrombosis. *Blood*. 2013;122(13):2176–2184.

23. Arellano-Rodrigo E, Alvarez-Larrán A, Reverter JC, et al. Increased platelet and leukocyte activation as contributing mechanisms for thrombosis in essential thrombocythemia and correlation with the JAK2 mutational status. *haematologica*. 2006;91(2):169–175.

24. Falanga A, Marchetti M, Evangelista V, et al. Polymorphonuclear leukocyte

activation and hemostasis in patients with essential thrombocythemia and polycythemia vera. *Blood*. 2000;96(13):4261–4266.

25. Sano S, Wang Y, Yura Y, et al. JAK2V617F-Mediated Clonal Hematopoiesis Accelerates Pathological Remodeling in Murine Heart Failure. *JACC Basic Transl. Sci*. 2019;4(6):684–697.
26. Kimishima Y, Misaka T, Yokokawa T, et al. Clonal hematopoiesis with JAK2V617F promotes pulmonary hypertension with ALK1 upregulation in lung neutrophils. *Nat. Commun*. 2021;12.:
27. Wang W, Liu W, Fidler T, et al. Macrophage Inflammation, Erythrophagocytosis and Accelerated Atherosclerosis in Jak2V617F Mice. *Circ. Res*. 2018;123(11):e35–e47.
28. Barboza MA, Chiquete E, Arauz A, et al. A practical score for prediction of outcome after cerebral venous thrombosis. *Front. Neurol*. 2018;9:882.
29. Jickling GC, Liu D, Ander BP, et al. Targeting neutrophils in ischemic stroke: translational insights from experimental studies. *J. Cereb. Blood Flow Metab*. 2015;35(6):888–901.
30. Desilles J-P, Syvannarath V, Ollivier V, et al. Exacerbation of Thromboinflammation by Hyperglycemia Precipitates Cerebral Infarct Growth and Hemorrhagic Transformation. *Stroke*. 2017;48(7):1932–1940.
31. Santisakultarm TP, Paduano CQ, Stokol T, et al. Stalled cerebral capillary blood flow in mouse models of essential thrombocythemia and polycythemia vera revealed by in vivo two-photon imaging. *J. Thromb. Haemost*. 2014;12(12):2120–2130.
32. Hasan S, Lacout C, Marty C, et al. JAK2V617F expression in mice amplifies early hematopoietic cells and gives them a competitive advantage that is hampered by IFN α . *Blood*. 2013;122(8):1464–1477.
33. Bourrienne M-C, Loyau S, Benichi S, et al. A Novel Mouse Model for Cerebral Venous Sinus Thrombosis. *Transl. Stroke Res*. 2021;
34. Egashira Y, Shishido H, Hua Y, Keep RF, Xi G. A new grading system based on magnetic resonance imaging in a mouse model of subarachnoid hemorrhage. *Stroke J. Cereb. Circ*. 2015;46(2):582–584.
35. Li M, Lin C, Leso A, Nefedova Y. Quantification of Citrullinated Histone H3 Bound DNA for Detection of Neutrophil Extracellular Traps. *Cancers*. 2020;12(11):3424.

36. Li S, Liu K, Gao Y, et al. Prognostic value of systemic immune–inflammation index in acute/subacute patients with cerebral venous sinus thrombosis. *Stroke Vasc. Neurol.* 2020;5(4):368–373.
37. Khoury JD, Solary E, Abla O, et al. The 5th edition of the World Health Organization Classification of Haematolymphoid Tumours: Myeloid and Histiocytic/Dendritic Neoplasms. *Leukemia.* 2022;36(7):1703–1719.
38. Sales C, Wijeratne T, Lucero A. Is JAK2-Mutation Associated with Extensive Clot Burden in Cerebral Venous Thrombosis. *Ann Clin Case Rep.* 2021;6:1911.
39. Schaller B, Graf R. Cerebral Venous Infarction: The Pathophysiological Concept. *Cerebrovasc. Dis.* 2004;18(3):179–188.
40. Capecchi M, Abbattista M, Martinelli I. Cerebral venous sinus thrombosis. *J. Thromb. Haemost.* 2018;16(10):1918–1931.
41. Guy A, Helzy K, Mansier O, et al. Platelet function studies in myeloproliferative neoplasms patients with Calreticulin or JAK2V617F mutation. *Res. Pract. Thromb. Haemost.* 2023;7(2.):
42. Falanga A, Marchetti M, Vignoli A, Balducci D, Barbui T. Leukocyte-platelet interaction in patients with essential thrombocythemia and polycythemia vera. *Exp. Hematol.* 2005;33(5):523–530.
43. Swystun LL, Liaw PC. The role of leukocytes in thrombosis. *Blood.* 2016;128(6):753–762.
44. Lisman T. Platelet–neutrophil interactions as drivers of inflammatory and thrombotic disease. *Cell Tissue Res.* 2018;371(3):567–576.
45. Guy A, Garcia G, Gourdou-Latyszenok V, et al. Platelets and neutrophils cooperate to induce increased neutrophil extracellular trap formation in JAK2V617F myeloproliferative neoplasms. *J. Thromb. Haemost.* 2023;0(0.):
46. Jin J, Qiao S, Liu J, et al. Neutrophil extracellular traps promote thrombogenicity in cerebral venous sinus thrombosis. *Cell Biosci.* 2022;12.:
47. Ed Rainger G, Chimen M, Harrison MJ, et al. The role of platelets in the recruitment of leukocytes during vascular disease. *Platelets.* 2015;26(6):507–520.
48. De Meyer SF, Denorme F, Langhauser F, et al. Thromboinflammation in stroke brain damage. *Stroke.* 2016;47(4):1165–1172.
49. Ding J, Song B, Xie X, et al. Inflammation in Cerebral Venous Thrombosis. *Front. Immunol.* 2022;13.:
50. Hu S, Lee H, Zhao H, Ding Y, Duan J. Inflammation and Severe Cerebral

Venous Thrombosis. *Front. Neurol.* 2022;13.:

51. Dentali F, Ageno W, Rumi E, et al. Cerebral venous thrombosis and myeloproliferative neoplasms: results from two large databases. *Thromb. Res.* 2014;134(1):41–43.
52. Gangat N, Guglielmelli P, Betti S, et al. Cerebral venous thrombosis and myeloproliferative neoplasms: A three-center study of 74 consecutive cases. *Am. J. Hematol.* 2021;96(12):1580–1586.
53. Martinelli I, De Stefano V, Carobbio A, et al. Cerebral vein thrombosis in patients with Philadelphia-negative myeloproliferative neoplasms An European Leukemia Net study. *Am. J. Hematol.* 2014;89(11):E200–E205.
54. Simaan N, Molad J, Honig A, et al. Characteristics of patients with cerebral sinus venous thrombosis and JAK2 V617F mutation. *Acta Neurol. Belg.* 2022;
55. Guadall A, Lesteven E, Letort G, et al. Endothelial cells harbouring the JAK2V617F mutation display pro-adherent and pro-thrombotic features. *Thromb. Haemost.* 2018;118(09):1586–1599.
56. Guy A, Gourdou-Latyszenok V, Lay NL, et al. Vascular endothelial cell expression of JAK2V617F is sufficient to promote a pro-thrombotic state due to increased P-selectin expression. *Haematologica.* 2019;104(1):70–81.
57. De Grandis M, Cambot M, Wautier M-P, et al. JAK2V617F activates Lu/BCAM-mediated red cell adhesion in polycythemia vera through an EpoR-independent Rap1/Akt pathway. *Blood.* 2013;121(4):658–665.
58. Poisson J, Tanguy M, Davy H, et al. Erythrocyte-derived microvesicles induce arterial spasms in JAK2V617F myeloproliferative neoplasm. *J. Clin. Invest.* 2020;130(5):2630–2643.
59. Zhao B, Mei Y, Cao L, et al. Loss of pleckstrin-2 reverts lethality and vascular occlusions in JAK2^{V617F}-positive myeloproliferative neoplasms. *J. Clin. Invest.* 2018;128(1):125–140.
60. Mansier O, Kilani B, Guitart AV, et al. Description of a knock-in mouse model of JAK2V617F MPN emerging from a minority of mutated hematopoietic stem cells. *Blood.* 2019;134(26):2383–2387.
61. Etheridge SL, Roh ME, Cosgrove ME, et al. JAK2V617F-positive endothelial cells contribute to clotting abnormalities in myeloproliferative neoplasms. *Proc. Natl. Acad. Sci. U. S. A.* 2014;111(6):2295–2300.

Appendix

Aude Triquenot Bagan^{*1}, Véronique Le Cam Duchez^{°1}, Isabelle Crassard^{*2}, Ludovic Drouet^{°2}, Marianne Barbieux-Guillot^{*3}, Raphaël Marlu^{°3}, Emmanuelle Robinet-Borgomino^{*4}, Pierre-Emmanuel Morange^{°4}, Valérie Wolff^{*5}, Lelia Grunebaum^{°5}, Frédéric Klapczynski^{*6}, Elisabeth André-Kerneis^{°6}, Fernando Pico^{*7}, Brigitte Martin-Bastenaire^{°7}, Emmanuel Ellie^{*8}, Fanny Menard^{°8}, François Rouanet^{*9}, Geneviève Freyburger^{°9}, Gaëlle Godenèche^{*10}, Hong-An Allano^{°10}, Thierry Moulin^{*11}, Guillaume Mourey^{°11}, Laurent Derex^{*12}, Micheline Berruyer^{°12}, Gwénaëlle Runavot^{*13}, Catherine Trichet^{°13}, Fausto Viader^{*14}, Agnès Le Querrec^{°14}, Thomas Tarek Husein^{*15}, Sophie Cluet-Dennetiere^{°15}, Francisco Macian-Montoro^{*16}, Magali Donnard^{°16}, Benoît Guillon^{*17}, Catherine Ternisien^{°17}, Mathieu Zuber^{*18}, Sophie Laplanche^{°18}, Philippe Tassan^{*19}, Jean-Yves Peeltier^{°19}, Sandrine Canaple^{*20}, Bertrand Roussel^{°20}, Nicolas Gaillard^{*21}, Emilie Scavazza^{°21}.

* Department of Neurology, ° Department of Biological Hematology

Affiliations:

¹ CHU Rouen, F-76000 Rouen, France ; ² Lariboisière University Hospital, F-75010 Paris, France ; ³ Grenoble University Hospital, F-38000 Grenoble, France ; ⁴ Marseille University Hospital, F-13000 Marseille, France ; ⁵ Strasbourg University Hospital, F-67000 Strasbourg, France ; ⁶ Meaux Hospital, F-77100 Meaux, France ; ⁷ Versailles Hospital, F-78000 Versailles, France ; ⁸ Bayonne Hospital, F-64100 Bayonne, France ; ⁹ Bordeaux University Hospital, F-33000 Bordeaux, France ; ¹⁰ La Rochelle Hospital, F-17000 La Rochelle, France ; ¹¹ Besançon University Hospital, F-25000 Besançon, France ; ¹² Lyon University Hospital, F-69000 Lyon, France ; ¹³ Argenteuil Hospital, F-95100 Argenteuil, France ; ¹⁴ Caen University Hospital, F-14000 Caen, France ; ¹⁵ Compiègne Hospital, F-60200 Compiègne, France ; ¹⁶ Limoges University Hospital, F-87000 Limoges, France ; ¹⁷ Nantes University Hospital, F-44000 Nantes, France ; ¹⁸ Saint Joseph Hospital, F-75001 Paris, France ; ¹⁹ Poissy-Saint-Germain Hospital, F-78300 Poissy, France ; ²⁰ Amiens University Hospital, F-80000 Amiens, France ; ²¹ Perpignan Hospital, F-66100 Perpignan, France.

Table

Table 1: Characteristics of CVST patients according to Jak2^{V617F} mutation status.

	JAK2 ^{V617F} -negative CVST (n=207)	JAK2 ^{V617F} -positive CVST (n=9)	p
Age	39 [28-51]	42 [24-75]	0.45
Male/Female	70/137	0/9	0.033
BMI (kg/m²)	25.6 [22.5-29]	23.6 [21.5-27.2]	0.27
Mode of onset			
Acute	73/207 (35%)	3/9 (33%)	0.90
Subacute	118/207 (57%)	6/9 (67%)	0.56
Chronic	16/207 (8%)	0/9 (0%)	1
Clinical findings			
Isolated intracranial hypertension	105/207 (50.7%)	6/9 (66.6%)	0.5
Focal deficits	87/207 (42%)	2/9 (22.2%)	0.31
Encephalopathy	13/207 (6.2%)	1/9 (11.1%)	0.46
Acquired thrombophilia			
Antiphospholipid syndrome	1/81 (12%)	0/9 (0%)	1
Hormonal (OC and/or pregnancy*)	101/207 (48.7%)	4/9 (44.4%)	1
Systemic disorders §	21/207 (10.1%)	0/9 (0%)	0.60
Extra-cerebral neoplasia	6/207 (2.8%)	0/9 (0%)	1
Inherited thrombophilia			
Protein C deficiency	3/192 (1.6%)	0/9 (0%)	1
Protein S deficiency	8/191 (4.2%)	0/9 (0%)	1
Antithrombin deficiency	3/187 (1.6%)	0/9 (0%)	1
Factor V Leiden	15/142 (11.2%)	0/6 (0%)	0.6
Factor II G20210A	20/167 (11.9%)	1/9 (11.1%)	0.93
Local risk factors #	30/207 (14.4%)	1/9 (11.1%)	1
Thrombosed sinuses/veins			
Superior Sagittal Sinus	96/207 (46.3%)	6/9 (66.6%)	0.31
Straight Sinus	26/207 (12.5%)	3/9 (33.3%)	0.10
Lateral Sinus	119/207 (57.4%)	6/9 (66.6%)	0.73
Deep Venous System	13/207 (6.2%)	1/9 (11.1%)	0.45
Cortical Veins	86/207 (41.5%)	5/9 (55.5%)	0.49
Number of sinus involved	2 [1-3]	3 [1.5-4]	0.23
Combined Sinus/Vein	74/207 (35.7%)	6/9 (66.6%)	0.079
Parenchymal lesions			
Ischemic	78/207 (37.6%)	4/9 (44.4%)	0.73
Ischemic	26/78 (33.3%)	2/4 (50%)	0.60
Hemorrhagic	27/78 (34.6%)	1/4 (25%)	1
Both	25/78 (32%)	1/4 (25%)	1
Biological findings			
Haemoglobin, g/dL	13.7 [12.7-15]	14.1 [13.3-15.5]	0.45
Haematocrit, %	41 [38.5-44]	41.7 [40-53]	0.23
WBC count, x10 ⁹ /L	9 [7-11.3]	13.3 [8.4-19.4]	0.062
Neutrophil count, x10 ⁹ /L	6.4 [4.5-8.7]	8 [5.3-11.1]	0.055
Platelet count, x10 ⁹ /L	260 [208-317]	319 [222-443]	0.11
D-Dimers, ng/mL	968 [553-1545]	1205 [493-2043]	0.91
CRP	12 [6-28]	16 [7.5-35.5]	0.45
Fibrinogen, g/L	4 [3.4-4.7]	4.1 [3.5-4.9]	0.74
Myeloperoxidase (ng/mL)	14.7 [9-22.4]	19.7 [15-26]	0.094
SII index	923 [531-1692]	1664 [1066-1989]	0.019
Outcome (mRS, 3 months follow-up)			
<2	163/190 (85.7%)	7/9 (77.7%)	0.62
≥2	21/190 (11%)	1/9 (11.1%)	1
Death	6/190 (3.1%)	1/9 (11.1%)	0.28

Results are expressed as median [IQR 25-75] or n (percentage,%). CVST: Cerebral Venous Sinus Thrombosis; BMI: Body Mass Index; mRS: modified Rankin Scale; OC: oestrogen contraceptive. *: 3 cases of pregnancy-related CVST; \$: Systemic disorders include Behçet disease, rheumatologic or connective tissue disease, vasculitis, sarcoidosis. #: Local risk factors include trauma, arteriovenous malformation, paracranial infection. Quantitative data were compared using Mann–Whitney’s t test. Qualitative data were analysed by Chi-square test.

Figures

Figure 1: *Jak2*^{V617F} mice showed an enhanced early endothelial adhesion of leukocyte and platelet in cerebral veins after CVST.

(A) Intravital microscopy imaging of venous brain network from *Jak2*^{WT} and *Jak2*^{V617F} mice representing superior sagittal sinus (SSS) and cortical venules (CtV) labelled with Dextran 2mKDa (green). Scale bar=200 μ m. (B) In sham-operated mice (left panel), sparse marginating leukocytes and platelets (Rhodamine 6G, red) were found in *Jak2*^{V617F} and *Jak2*^{WT} mice. Two hours after CVST, adhesion and accumulation of platelets and leukocytes increased in both *Jak2*^{V617F} and *Jak2*^{WT} mice (right panel). Dextran imaging showed black segments within venules (white arrow), indicating a disruption in blood flow and formation of new thrombi. (C) Median of fluorescence intensity of rhodamine 6G-labeled platelets and leukocytes as a marker of thrombosis burden in CtV. Results are expressed as mean \pm SD (n=5 per group). Data were analysed using Kruskal-Wallis test. *: p<0.05, **: p<0.01. (D) Labelling of neutrophils (Ly6G, pink) (lower panel) and vessels (Dextran 2mKDa, green) (upper panel) showed that neutrophils were mainly involved in endothelial adhesion in *Jak2*^{V617F} mice. Scale bars: 25 μ m.

Figure 2: *Jak2*^{V617F} mice displayed more CVST-related haemorrhagic lesions at day 1.

(A) Representative serial coronal T2-weighted images from *Jak2*^{WT} and *Jak2*^{V617F} mice, one day after CVST (D1) induction demonstrating localized ischemia (white asterisk) and/or ICH (black arrow) in cortical parenchyma. (B) Brain lesions volumes (ischemic and haemorrhagic) determined from coronal T2-weighted images from *Jak2*^{WT} and *Jak2*^{V617F} mice at D1, n=5 per group. (C) Quantification of haemoglobin brain content at D1 after CVST, *: p<0.05 (t test) n=6 per group. (D) Brain slices from *Jak2*^{V617F} and *Jak2*^{WT} mice showing different pattern of ICH severity after CVST (no ICH, type 1: localised ICH, type 2: diffuse ICH). (E) Incidence of severe ICH (i.e. type 2) was significantly increased in *Jak2*^{V617F} mice compared to *Jak2*^{WT} mice at D1 post-CVST (n=17 and 12 per group, respectively). In figures 1B and 1E, data were

analysed using Mann–Whitney’s t test. In figure 1D, data were analysed by Chi-square test. *: $p < 0.05$.

Figure 3: BBB leakage is exacerbated in $Jak2^{V617F}$ mice after CVST

(A) After CVST, staining for IgG (pink); blood vessel (GLUT-1, green); red blood cells (RBC, white) and cell nuclei (DAPI, cyan) in brain sections from $Jak2^{WT}$ and $Jak2^{V617F}$ mice showed IgG extravasation in hemorrhagic and non-hemorrhagic areas. Scale bars: 25 μm . (B) Bar graph indicated quantification of IgG content (mean \pm SD) in whole brain from $Jak2^{WT}$ and $Jak2^{V617F}$ mice in sham and CVST conditions at day 1, $n=5-6$ per group. Data were analysed using Kruskal-Wallis test followed by post hoc Dunn’s test. *: $p < 0.05$.

Figure 4: Brain neutrophil infiltration is increased in $Jak2^{V617F}$ mice after CVST.

(A) Representative images of coronal brain sections taken through the area of damage from $Jak2^{WT}$ and $Jak2^{V617F}$ mice after CVST at day 1 (D1). Hematoxylin and eosin (H&E) staining showed the presence of hemorrhagic (H) lesions and non-hemorrhagic cortical parenchyma (no H) in dotted rectangles. Scale bar: 500 μm . (B) Corresponding brain images of staining for myeloperoxidase (MPO, red); cell nuclei (DAPI, cyan) and red blood cells (RBC, yellow) in “no H” (upper panel) and “H” area (lower panel) from $Jak2^{WT}$ and $Jak2^{V617F}$ mice after CVST at D1. Scale bars: 50 μm . (C) Bar graph indicated number of neutrophils within “no H” cortical parenchyma in sham and CVST mice ($Jak2^{WT}$ and $Jak2^{V617F}$), $n=10$ per group. Bar graphs indicated quantification of PF4 (D) and MPO (E) contents in whole brain from $Jak2^{WT}$ and $Jak2^{V617F}$ mice at D1 in sham-operated and CVST mice, $n=5-6$ per group. All results are expressed as mean \pm SD. Data were analysed by Kruskal-Wallis test followed by post hoc Dunn’s test. *: $p < 0.05$, ***: $p < 0.01$.

Figure 5: Increased formation of platelet-neutrophil aggregates in $Jak2^{V617F}$ mice

(A) Circulating platelet-neutrophil aggregates (PNA); and neutrophil CD11b expression (B) are measured in $Jak2^{WT}$ and $Jak2^{V617F}$ mice at baseline, and at day 1 (D1) in sham-operated and CVST mice. Myeloperoxidase (MPO) (C) and

citrullinated histone H3 bound DNA (D) plasma levels are measured in the same conditions. Platelet-neutrophil aggregates (PNAs) were calculated from Ly6G positive events as the percentage of neutrophils. Results are expressed as mean±SD, n=5-6 per group. Data were analysed by Kruskal-Wallis test followed by post hoc Dunn's test. *: p<0.05. **: p<0.01.

Figure 6: Platelet activation in *Jak2*^{WT} and *Jak2*^{V617F} mice

Activation of αIIbβ3 integrin using binding of labelled-fibrinogen (A) and platelet P-Selectin expression (B) are measured in platelets using flow cytometry in both *Jak2*^{WT} and *Jak2*^{V617F} mice at baseline and at day 1 (D1) after sham-surgery or CVST (C) Bar graph indicating plasma levels of soluble P-Selectin (sP-Sel). Results are expressed as mean±SD, n=7-8 per group. Data were analysed using Kruskal-Wallis test followed by post hoc Dunn's test. *: p<0.05. **: p<0.01.

Figure 1

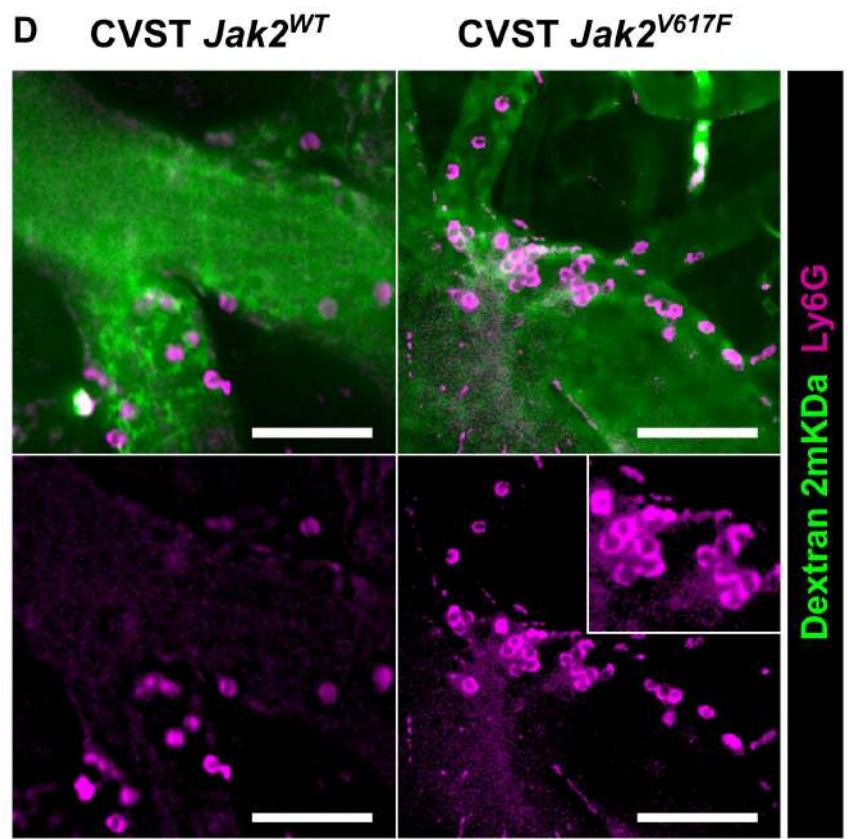
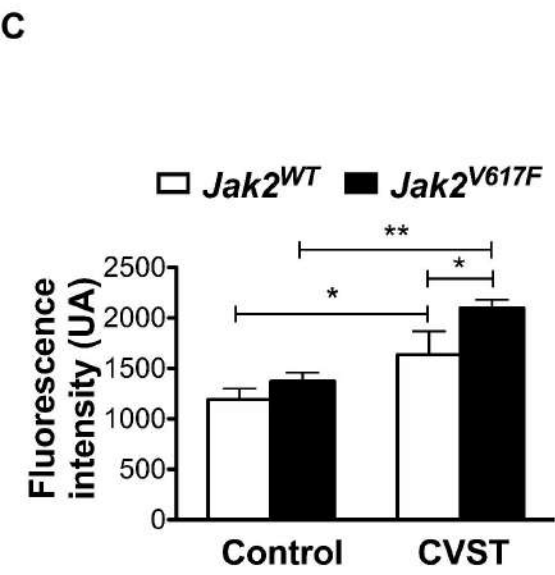
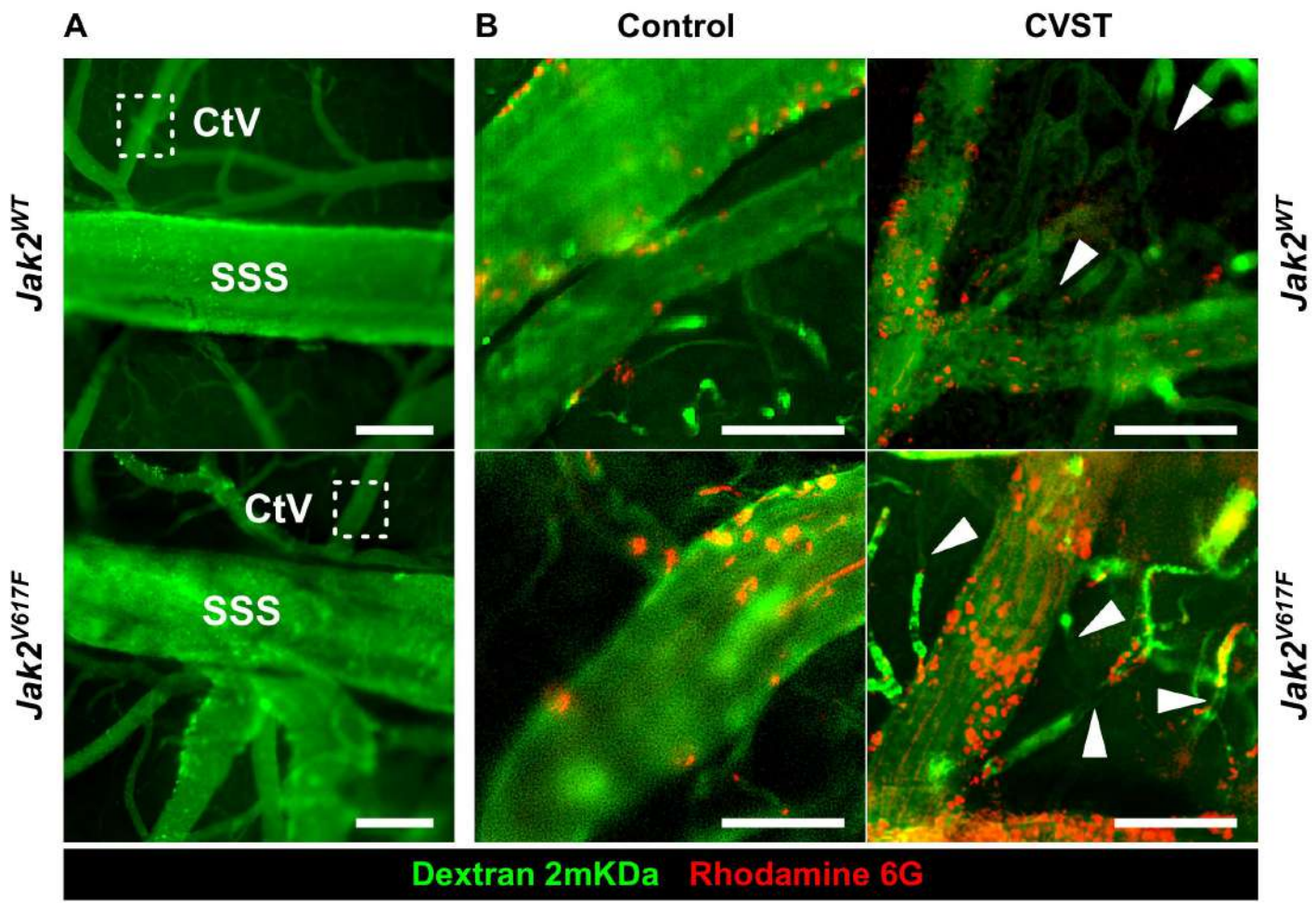


Figure 2

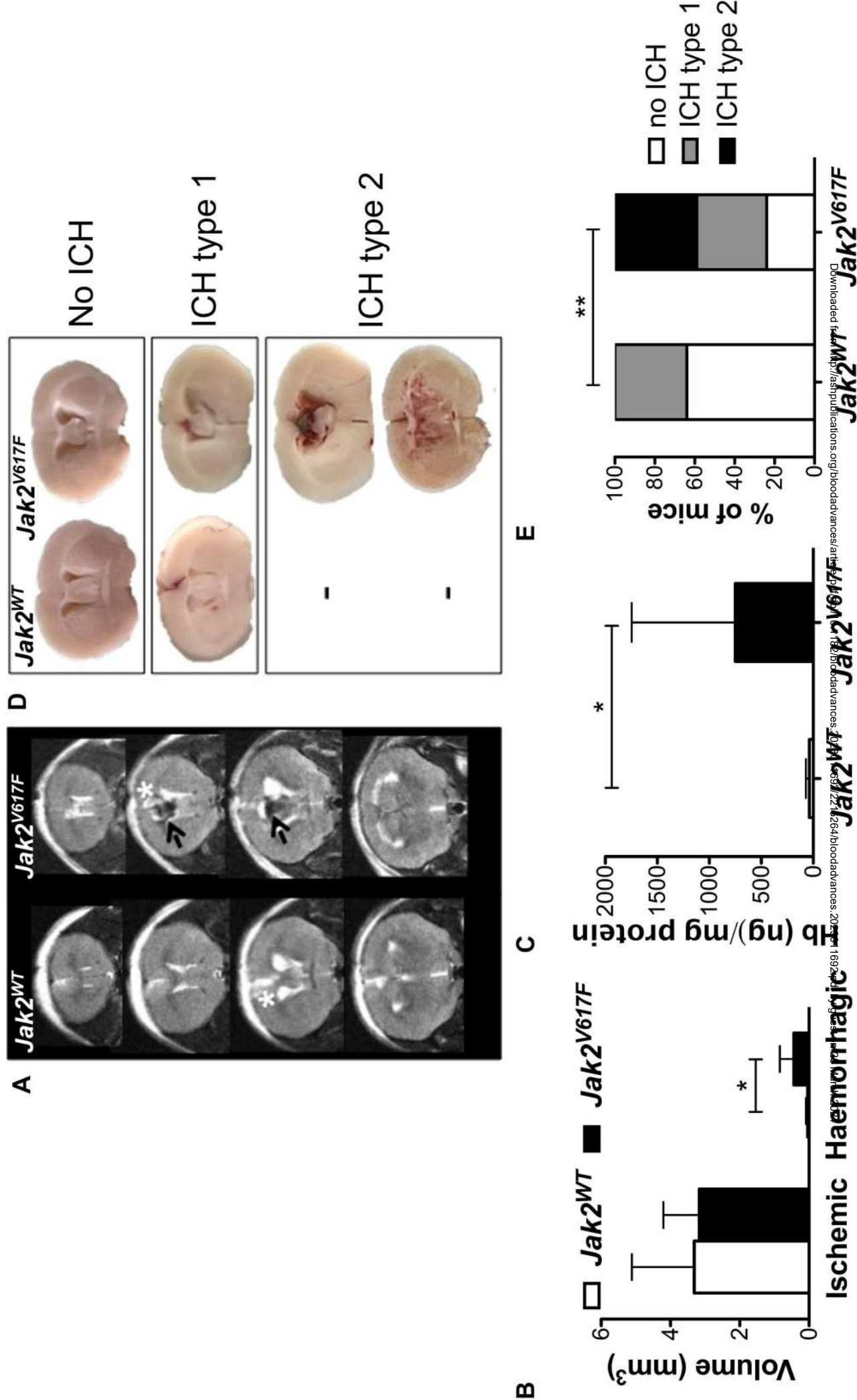
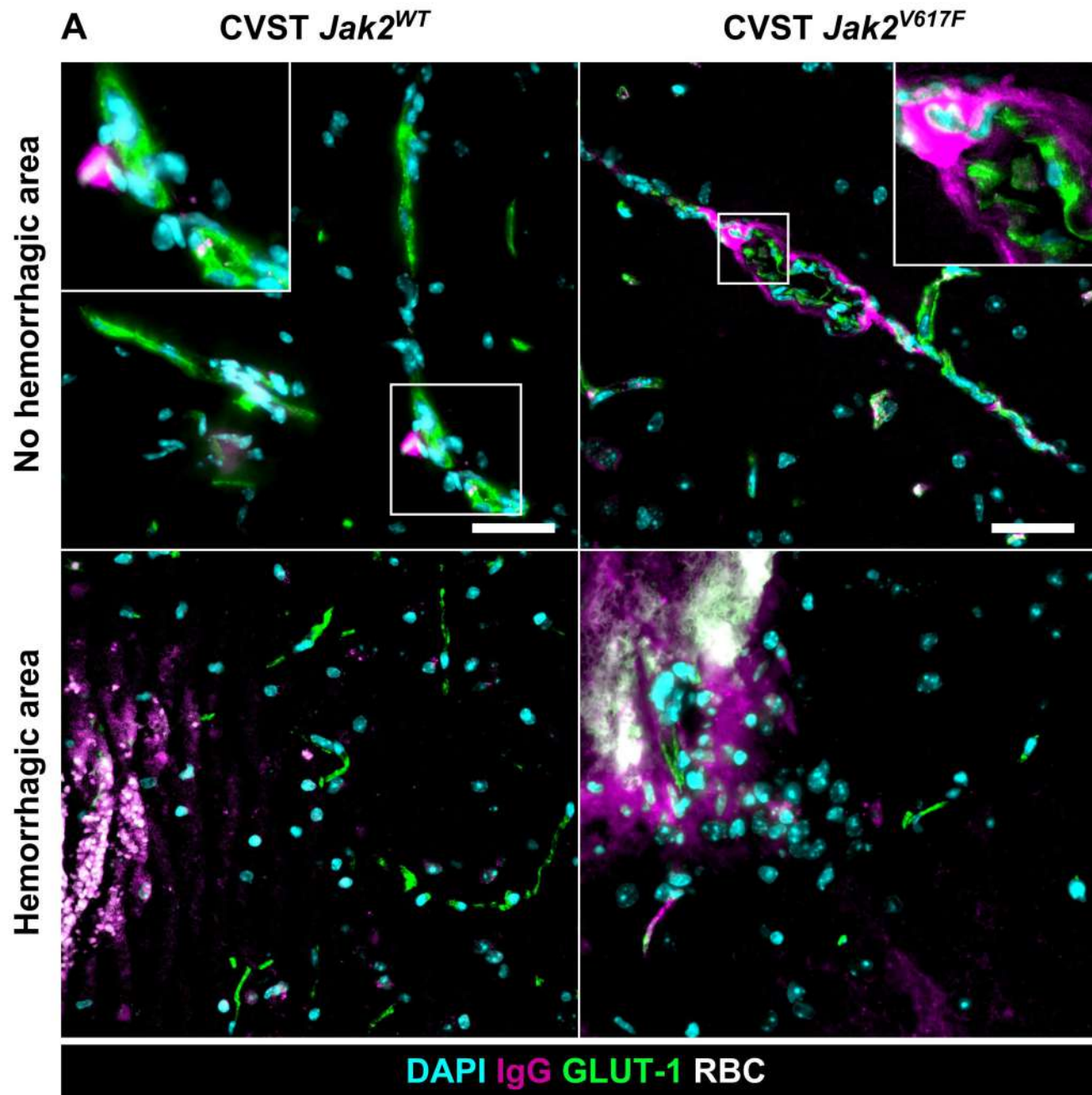


Figure 3



B

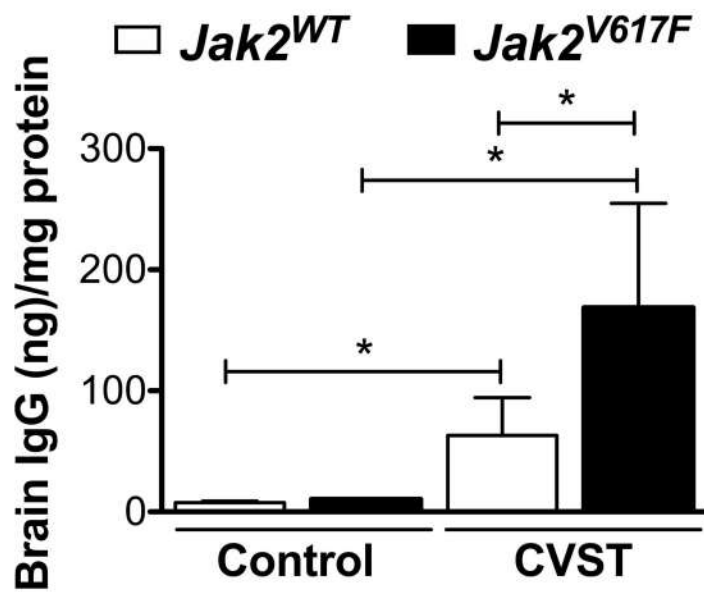


Figure 4

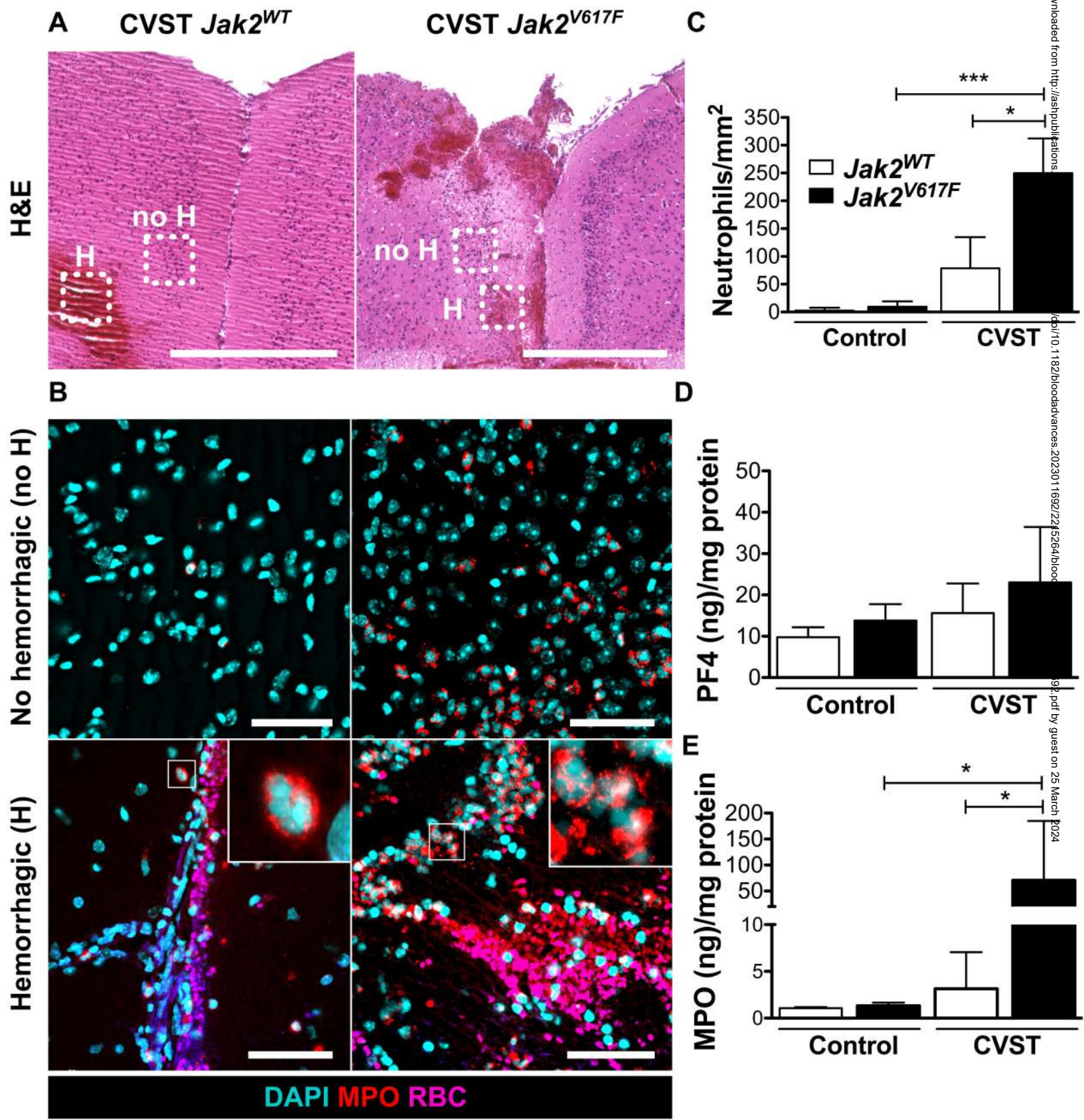
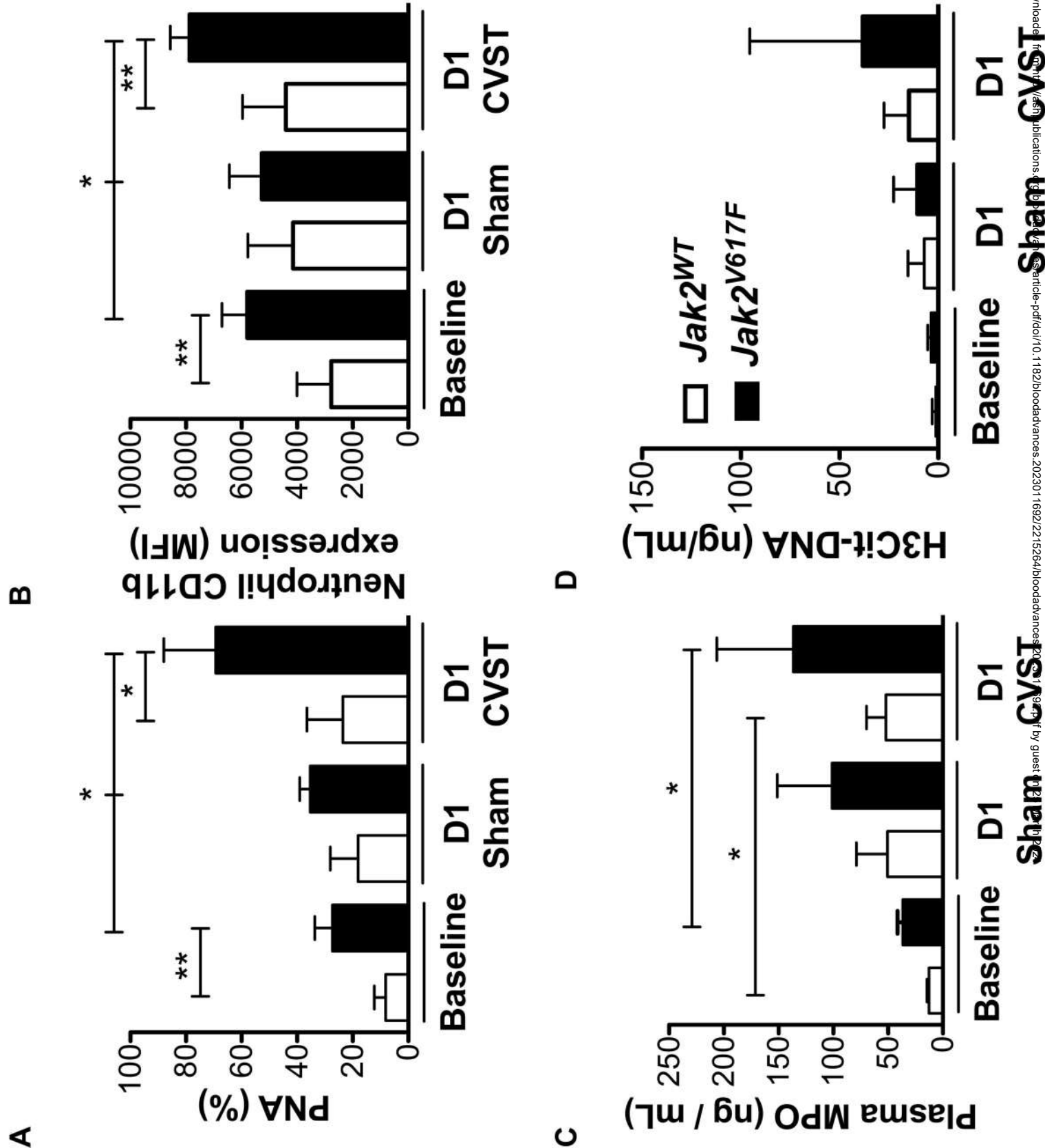
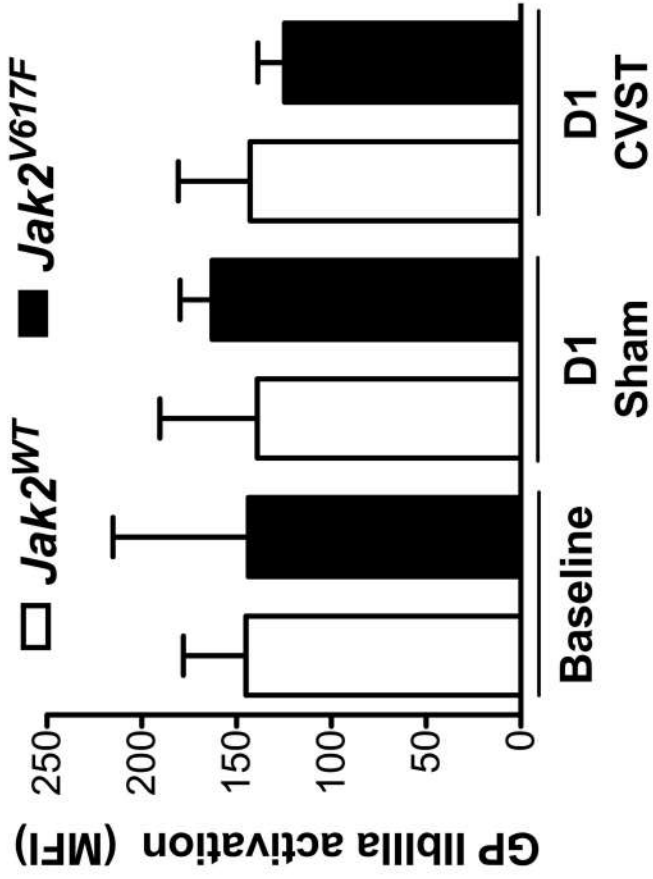


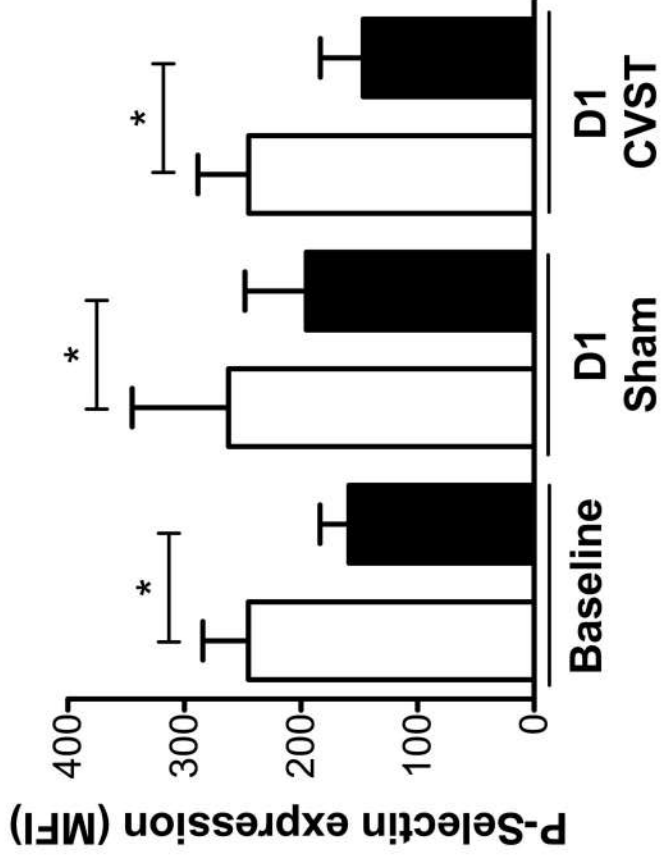
Figure 5



A



B



C

